

352 **A Appendix: OODEEL’s Visualization and Benchmarking Features**

353 **Visualization** OODEEL also comes with quality-of-life features. The first feature includes three
 354 useful visualizations that are often used in OOD detection research: Histogram plots for ID and
 355 OOD scores, ROC curve, and t-SNE plot of the model’s penultimate layer. The first two are used
 356 to assess the performance of a detector, and the last is often used to qualitatively evaluate the
 357 discriminating capabilities of a given neural network, which often prefigures its Post-hoc OOD
 358 detection performances. Examples of these visualizations are found in Figure 9

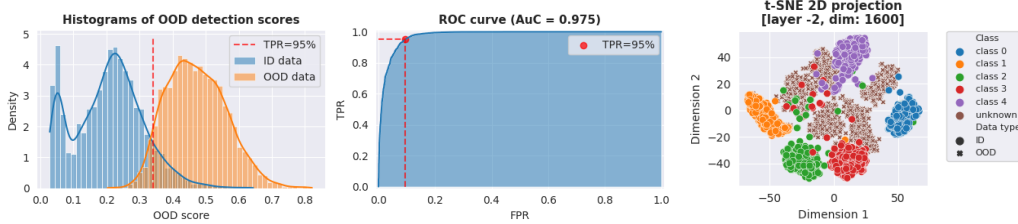


Figure 9: Visualization tools provided by Oodeel. **From left to right:** Histograms and KDE plots for ID vs OOD scores, ROC curve, and t-SNE visualization of a model’s feature space.

359 **Benchmarking** The last feature is a benchmarking utility that allows for easy testing of the per-
 360 formance of OODEEL’s detectors on OpenOOD benchmark. This feature comes with a clean
 361 configuration logic, checkpointing, and sharding capabilities, reducing the benchmarking hassle. It
 362 also records computational performance metrics, such as VRAM utilisation and execution time. The
 363 experiments can be tracked from the terminal through a `rich` interface, and logged to WeightsAndBi-
 364 ases (illustration of the interface in Figure 10). The benchmarking utility is part of another repository
 365 called `oodeel-benchmark`⁴ hosted on GitHub.

```
[11:40:44] Running [uid= df16d2cc] → cifar10 / cifar10_resnet20 / odin(react):none
[11:40:56] [mem] Fit           Δ= 0.0 MiB peak= 40.4 MiB time= 11.4s
[11:40:59] [mem] ID score     Δ= 0.0 MiB peak= 213.4 MiB time= 3.2s
[11:41:03] [mem] OOD cifar100  Δ= 0.0 MiB peak= 213.4 MiB time= 3.5s
[11:41:07] [mem] OOD tin      Δ= 0.0 MiB peak= 213.4 MiB time= 3.0s
[11:41:22] [mem] OOD mnist    Δ= 0.0 MiB peak= 213.4 MiB time= 14.9s
[11:41:36] [mem] OOD svhn     Δ= 0.0 MiB peak= 213.4 MiB time= 7.0s
[11:41:42] [mem] OOD texture   Δ= -0.0 MiB peak= 213.4 MiB time= 4.6s
[11:41:52] [mem] OOD places365 Δ= 0.0 MiB peak= 213.4 MiB time= 9.4s
[11:41:54] ✓ cifar10 | cifar10_resnet20 | odin:none → AUROC-near=0.820 AUROC-far=0.823 HM=0.821
```

Figure 10: Caption

366 **B Appendix: Details on the Benchmark Setting**

367 In this appendix, we provide a complete description of the hardware, software, datasets, models, and
 368 orchestration logic used in our out-of-distribution (OOD) detection benchmark. Our goal is to enable
 369 exact reproduction of all experiments.

370 **B.1 Compute Environment**

371 We ran all experiments on a single machine equipped with:

372 **Hardware**

373 • 2 × NVIDIA RTX 4090 GPUs (24 GB VRAM each)
 374 • CPU RAM: 128 GB

375 **Software**

⁴<https://github.com/deel-ai/oodeel-benchmark>

376 • Python 3.10, PyTorch 2.7.0, torchvision 0.22.0
 377 • OODEel library (dev branch, commit `ff4fa17`, will soon be merged)

378 **Runtime & Logging**
 379 • Wall-clock time: \approx 1 week on $2 \times$ RTX 4090
 380 • Batch size: 64 per GPU; peak VRAM \leq 20 GB
 381 • Metrics streamed to Weights & Biases (and available in “All runs” leaderboard from
 382 <https://oodeel-benchmark.streamlit.app/>)

383 **B.2 Repository & Benchmark Orchestration**

384 All code is available at <https://github.com/deel-ai/oodeel-benchmark>. We drive the full
 385 sweep with:

386 `python -m src.run --num-shards 2 --shard-index 0`

387 This script:

- 388 1. Loads every YAML in `configs/datasets/`, `configs/models/`, `configs/methods/`.
- 389 2. Forms the Cartesian product of (dataset, model, method, hyperparameters) configurations.
- 390 3. Shards the list via `-num-shards/-shard-index`.
- 391 4. Skips runs with existing `.parquet` outputs in `results/`.
- 392 5. Streams raw scores, AUROC, and TPR@5% FPR to W&B.

393 **B.3 Sweep Construction & Config Logic**

394 Each YAML file defines a flat key–value mapping:

- 395 • `configs/datasets/*.yaml`: list of near- and far-ood datasets for a given id dataset, model
 396 names.
- 397 • `configs/models/*.yaml`: architecture name, checkpoint source, feature-extraction lay-
 398 ers.
- 399 • `configs/methods/*.yaml`: detector type and hyperparameter grid.

400 The driver merges one file from each folder into a single run configuration. Sharding evenly slices
 401 this list across processes, and checkpointing ensures idempotent restarts.

402 **B.4 Datasets & Models Tested**

403 We follow the OpenOOD benchmark in pairing each in-distribution (ID) dataset with semantically
 404 *near* and *far* OOD test sets.

405 **CIFAR-10:**

- 406 • **Near-OOD:** CIFAR-10, Tiny ImageNet
- 407 • **Far-OOD:** MNIST, SVHN, Textures, Places365

408 **CIFAR-100:**

- 409 • **Near-OOD:** CIFAR-10, Tiny ImageNet
- 410 • **Far-OOD:** MNIST, SVHN, Textures, Places365

411 **ImageNet-1k:**

- 412 • **Near-OOD:** SSB-hard, NINCO
- 413 • **Far-OOD:** iNaturalist, Textures, OpenImage-O

414 **Model Architectures** We evaluate 11 models on CIFAR and 7 on ImageNet, including:

- 415 • **ResNets:** ResNet-18, ResNet-32, ResNet-50
- 416 • **VGG:** VGG11, VGG16, RepVGG-A0, RepVGG-A2
- 417 • **MobileNets:** MobileNet v2, MobileNet v3-Large

418 • **ShuffleNets:** ShuffleNet v2
419 • **Transformers:** ViT-B/16, Swin-Tiny
420 • **RegNet:** RegNetY-16GF

421 **B.5 OOD Detectors & Hyperparameter Sweeps**

422 We evaluate 12 base OOD detection methods (e.g. MSP, Energy, Mahalanobis, ODIN, DKNN, SHE,
423 VIM, ...) and for each base method construct variants as follows:

424 • **Logits-based variants:** with and without ReAct clipping, ASH, and SCALE transforma-
425 tions.
426 • **Feature-based variants:** with and without score aggregation over different feature layers.

427 This yields a total of 42 distinct method configurations. All hyperparameter search grids are specified
428 in the `configs/methods/` folder of the `odeel-benchmark` repository.

429 **B.6 Logging, Results & Reproducibility**

430 Each run writes a Parquet file in `results/` containing raw scores, AUROC, and TPR@5% FPR.
431 Visualizations are provided via console bars (Rich) and W&B dashboards. All code, exact commit
432 hashes, and example launch commands (including seed settings in `src/utils.py`) are publicly
433 available, ensuring full reproducibility.

434 **C Appendix: Complementary benchmark results**

435 In this section, we include complementary plots to the main document for CIFAR-100 and Far-OOD
436 experiments. This section is structured as the experiments section.

437 **C.1 Impact of the Model**

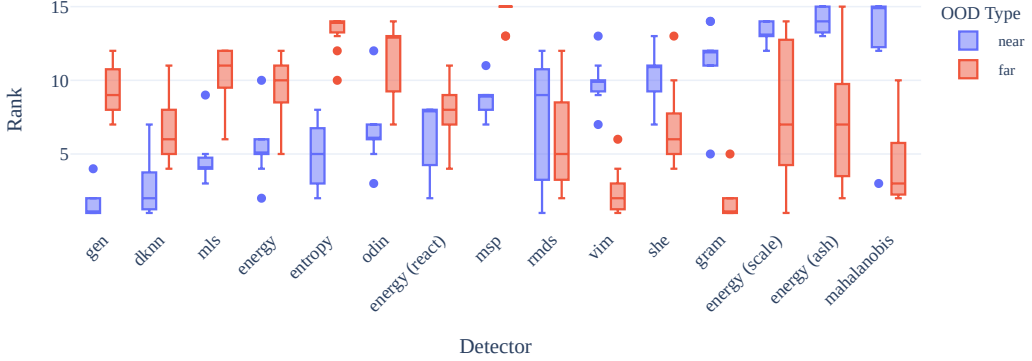


Figure 11: Box plots of the rank for each detector on CIFAR-100. Methods are sorted according to their mean rank on near-OOD. For CIFAR-100, the rank is very different for Near-OOD and Far-OOD, which corroborates the observation of the main paper that performances on Near and Far OOD do not always correlate.

438 We also report the Spearman rank correlation heatmap between the detectors' rank per model in
439 Figure 12 for CIFAR-10, CIFAR-100, and ImageNet. We can see that there is some correlation in
440 the rank of the detectors for CIFAR-10 and CIFAR-100, even if it is not high enough to alleviate the
441 need to test every detector on various models. For ImageNet, the correlation is significantly lower,
442 emphasizing this need even strongly.

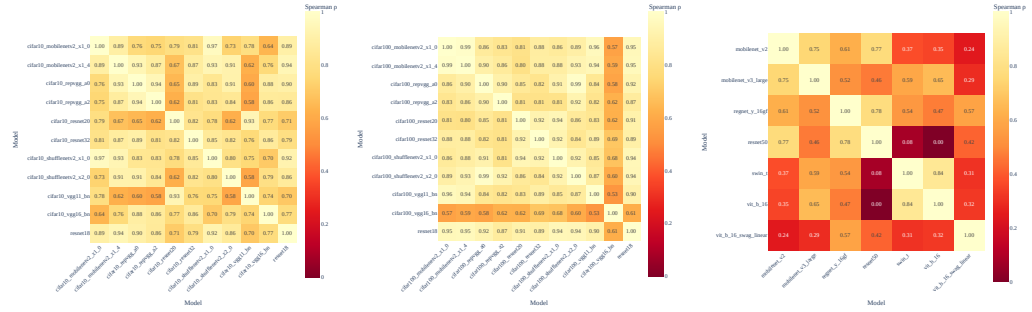


Figure 12: Spearman rank correlation between the AUROC of the detectors for each model. **From left to right:** CIFAR-10, CIFAR-100, ImageNet.

443 C.2 Impact of Layer-wise Score Aggregation

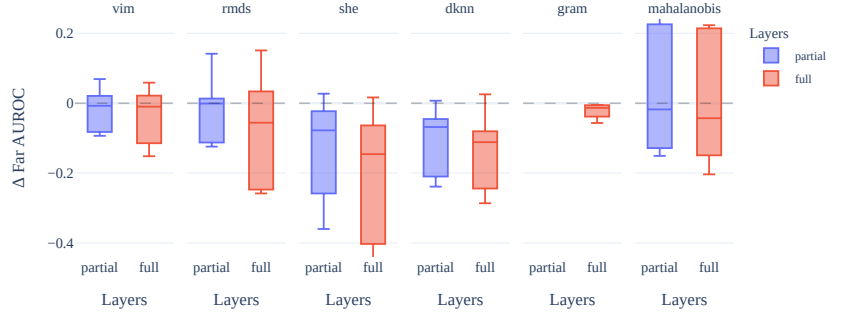


Figure 13: Box plot of the Δ in AUROC between feature-based detector applied on the penultimate layer and either a subset of the internal layers (partial) or all internal layers (full) for **ImageNet Far-OOD**.

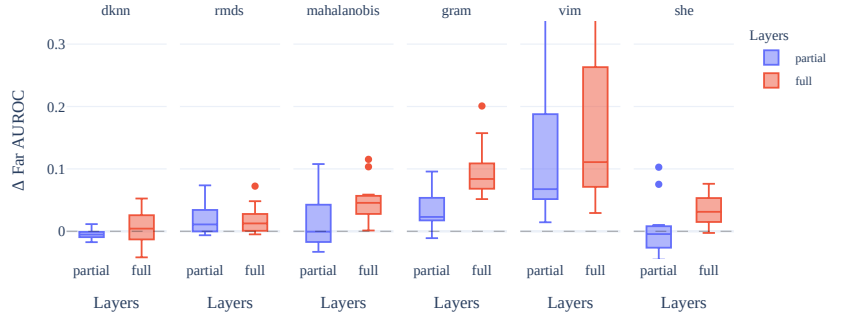


Figure 14: Box plot of the Δ in AUROC between feature-based detector applied on the penultimate layer and either a subset of the internal layers (partial) or all internal layers (full) for **CIFAR-10 Far-OOD**.

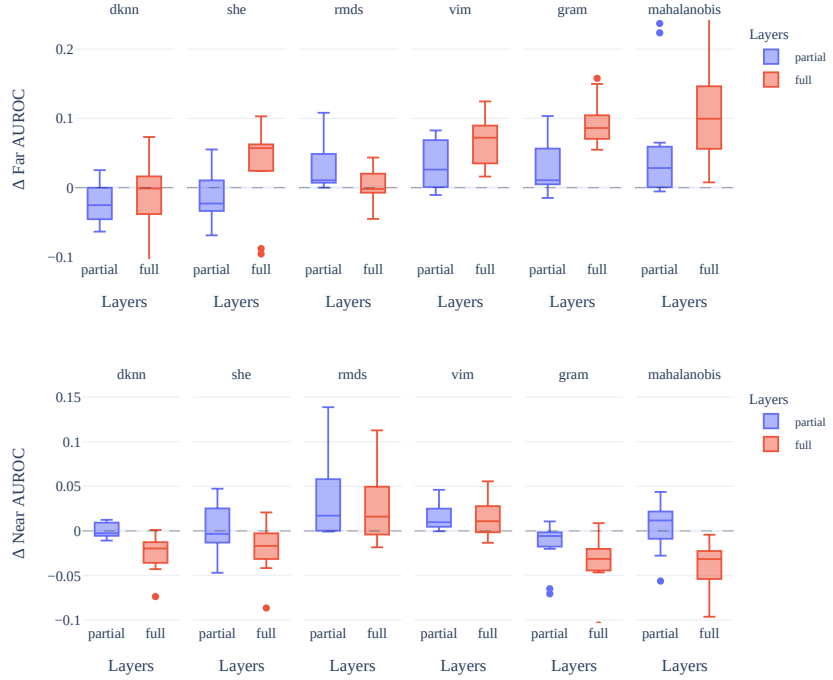


Figure 15: Box plot of the Δ in AUROC between feature-based detector applied on the penultimate layer and either a subset of the internal layers (partial) or all internal layers (full) for **top**: CIFAR-100 Near-OOD, **bottom**: CIFAR-100 Far-OOD

444 C.3 Impact of Activation Shaping

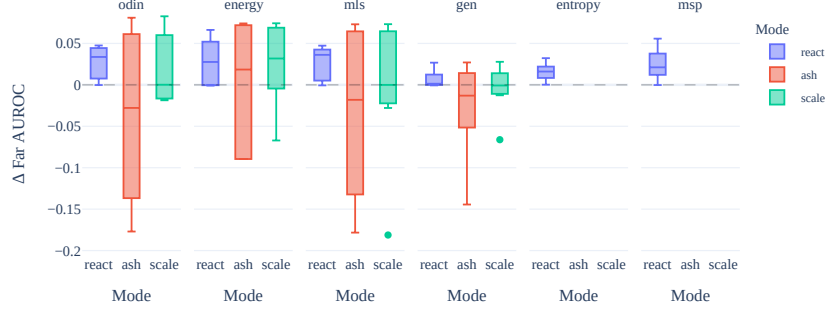


Figure 16: Box plot of the Δ in AUROC between logit-based detectors and their augmentation with activation-shaping techniques (ReAct, SCALE, and ASH) for **ImageNet Far-OOD**.

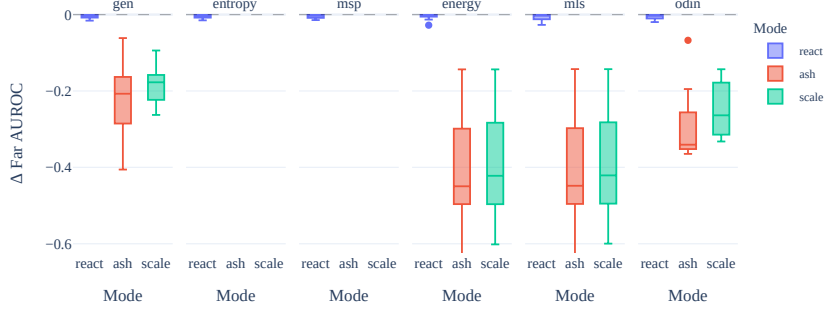


Figure 17: Box plot of the Δ in AUROC between logit-based detectors and their augmentation with activation-shaping techniques (ReAct, SCALE, and ASH) for **CIFAR-10 Far-OOD**.



Figure 18: Box plot of the Δ in AUROC between logit-based detectors and their augmentation with activation-shaping techniques (ReAct, SCALE, and ASH) for **top: CIFAR-100 Near-OOD, bottom: CIFAR-100 Far-OOD**. Interestingly, the effect of activation shaping on Far-OOD is quite beneficial for CIFAR-100 Far-OOD, whereas it is not for CIFAR-100 Near-OOD or CIFAR-10 Far-OOD.

445 **D Appendix: Sanity check of OODEEL detectors implementation by**
 446 **performance comparison with OpenOOD detectors**

447 To ensure the reliability of our OOD detection results using OODEEL, we conducted a sanity check
 448 by comparing our outcomes with those reported on the OpenOOD leaderboard. This validation step
 449 focused on both near-OOD detection tasks presented in Table 1.

450 Note that we obtain a significant improvement for the Gram method from OODEEL with respect
 451 to OpenOOD. It stems from a key implementation detail: in OODEEL, the Gram score relies on
 452 computing deviations based on quantiles (e.g., the 1st and 99th percentiles) of the features, whereas

453 OpenOOD uses the absolute minimum and maximum feature values. The use of quantiles in OODEEL
454 leads to a more robust formulation for outliers.

455 Globally, the obtained AUROC aligns with OpenOOD. The differences are mainly slight, with
456 OODEEL doing better than the OpenOOD implementation for 22 cases, equal for 4, and worse for
457 16 baselines. For a few exceptions, the difference is significant:

458 • OODEEL performs significantly better for Gram (three datasets), ODIN (CIFAR-10), and
459 SHE (CIFAR-10)
460 • OpenOOD performs significantly better for RMDS (CIFAR-10)

461 Except for Gram, when there is such a large discrepancy, it is only for one dataset. It provides
462 confidence in the correctness and robustness of our implementation.

Table 1: Comparison of **near-OOD** detection AUROC between OpenOOD and OODEEL. We used pretrained ResNet-18 for CIFAR-10 and CIFAR-100, and ResNet-50 for ImageNet.

Method	CIFAR-10		CIFAR-100		ImageNet	
	OpenOOD	OODEEL	OpenOOD	OODEEL	OpenOOD	OODEEL
MLS	87.52	87.89	81.05	79.89	76.46	76.46
MSP	88.03	88.30	80.27	79.05	76.02	76.02
ODIN	82.87	87.72	79.90	79.72	74.75	75.73
GEN	88.20	89.15	81.31	80.13	76.85	77.71
SHE	81.54	83.16	78.95	77.86	73.78	72.61
Energy	87.58	87.98	80.91	79.80	75.89	75.89
ReAct	87.11	87.93	80.77	79.75	77.38	77.39
SCALE	82.55	82.48	80.99	79.78	81.36	81.36
ASH	75.27	79.99	78.20	79.61	78.17	79.63
DKNN	90.64	91.02	80.18	79.92	71.10	72.24
Mahalanobis	84.20	84.91	58.69	59.43	55.44	55.83
RMDS	89.80	86.82	80.15	79.22	76.99	76.32
VIM	88.68	87.34	74.98	74.30	72.08	72.64
Gram	58.66	88.73	51.66	70.50	61.70	70.72